J. Electrochem. Sci. Eng. **15(5)** (2025) 2698; http://doi.org/10.5599/jese.2698

Open Access : : ISSN 1847-9286
www.jESE-online.org

Original scientific paper

Porcine gelatine detection *via* electrochemical immunosensors utilizing green-synthesized cerium oxide nanoparticles from orange peel

Rafa Radithya Swara[1], Nazwa Alya Zahra[1], Dea Hasna Tsary[1], Biyas Aurora Nania Nevada[1], Elisabeth Nasya Dominika Setyawati Putri[2], Salma Nur Zakiyyah[1], Yohanes Susanto Ridwan[1,3], Yeni Wahyuni Hartati[1,4] and Irkham[1,4,✉]

[1]*Department Chemistry, Faculty of Mathematics and Natural Science, Universitas Padjadjaran, Jalan Raya Bandung-Sumedang Km 21 Jatinangor, Sumedang 45363, Indonesia*
[2]*Department of Biology, Faculty of Mathematics and Natural Sciences, Universitas Padjadjaran, Jalan Raya Bandung-Sumedang Km 21 Jatinangor, Sumedang 45363, Indonesia*
[3]*Directorate of Laboratory Management, Research Facilities, and Science and Technology Park, National Research and Innovation Agency, Republic of Indonesia, Jakarta 10340, Indonesia*
[4]*Study Center of Sensor and Green Chemistry, Faculty of Mathematics and Natural Science, Universitas Padjadjaran, Bandung 40132, Indonesia*

Corresponding author: ✉*irkham@unpad.ac.id*

Received: March 2, 2025; Accepted: July 9, 2025; Published: July 31, 2025

Abstract

Maintaining the safety and proper labelling of food products is vital for communities around the world. One of the primary concerns in food safety is the unintentional presence of porcine derivatives such as gelatine in food products. This issue could affect the labelling accuracy of food products, religious dietary observances, regulatory compliance, and public health. Electrochemical immunosensors address this issue by rapidly, portably, and especially with high sensitivity, detecting porcine gelatine. The electrode was modified with CeO_2 nanoparticles (NPs) synthesized via a green method using orange peel extract, which enhanced the immobilization of the bioreceptor on the electrode surface. Orange peel extract contains secondary metabolites that can act as stabilizing agents and prevent agglomeration during the synthesis process. The synthesized CeO_2 NPs show a cube morphology, producing an average particle size of 12 nm with 77.31 % crystallinity. The performance of green synthesized CeO_2 NPs modified electrode are successful for detecting porcine gelatine in solution and commercialized gelatine product, resulting in a limit of detection of 3.53 ppm. These results show the potential of green-synthesized CeO_2 NPs for an electrochemical immunosensor for detecting porcine products.

Keywords

Food ingredient; electrochemical sensing; screen printed electrode; nanoceria; plant extract

Introduction

Food adulteration, where unauthorized substances are added or substituted, poses a serious threat to both food quality and public health. This practice can involve substituting food items with lower-quality alternatives, adding artificial colorants or preservatives, and misrepresenting the origin of food products [1]. Deliberate tampering, often for economic gain, introduces harmful agents that go beyond traditional safety concerns. When harmful substances or inferior ingredients are added to food, the risk to consumers increases, leading to potential health issues. These can range from mild discomfort to severe conditions such as allergies, cancer, and neurological disorders. Economically motivated food fraud not only compromises the integrity of food but also jeopardizes consumer safety by introducing dangerous contaminants. Non-halal additives can be considered a form of food adulteration if they are added to food products without proper labelling or if they mislead consumers regarding the nature of the food. In the context of halal dietary laws, the inclusion of non-halal substances in food intended for Muslim consumers can be seen as a violation of their dietary restrictions and can be classified as adulteration. This is particularly relevant when such additives are not disclosed, leading to a misrepresentation of the food's compliance with halal standards [1]. For example, porcine gelatine is often used in many processed foods since it possesses excellent gelling, thickening, and stabilizing properties [2]. However, the inclusion potentially exposes consumers to harmful pathogens like Hepatitis E Virus [3] and Trichinella spiralis [4]. In addition to the health risks, the use of pork is particularly concerning in contexts where Halal standards must be upheld, as it is prohibited in such diets. Ensuring food products are free from such adulteration is critical for protecting both public health and the cultural dietary needs of many communities.

The detection of gelatine content in food products can be achieved by various methodologies, including liquid chromatography-tandem mass spectrometry [5], polymerase chain reaction [6,7], attenuated total reflectance-Fourier transform infrared [8], and enzyme-linked immunosorbent assay (ELISA), as being among the most specific and frequently employed [9]. However, those techniques are not without limitations, including prolonged analysis times, costly equipment and reagents, and an inability to be miniaturized [10]. Electrochemical-based biosensors present a viable alternative to overcome these limitations. These biosensors are analytical devices designed to measure specific target analytes in samples such as blood, urine, or other body tissues [11]. Central to biosensor functionality are bioreceptors that enable specific antigen-antibody interactions (immunosensor), utilizing components like porcine anti-gelatine and porcine gelatine. Electrochemical immunosensors provide cost-effectiveness, quick response times, user-friendliness, and the potential for developing portable and enabling the use of disposable electrodes. Disposable electrodes are essential in biosensing, as they help maintain sterility and prevent cross-contamination, ensuring analytical accuracy and user safety. Their single-use also minimizes surface fouling and simplifies workflows, making them ideal for food safety testing [12,13].

Additionally, to further emphasize the portability, screen-printed carbon electrodes (SPCE) are widely used due to their simplicity, having all three necessary electrode components in one single chip. However, SPCE is not inherently selective nor active enough for direct bioreceptor immobilization, leading to the necessity for surface modification of the electrodes to be able to be used in specific applications [14,15]. It has been reported that SPCEs can be modified with cerium oxide nanoparticles (CeO_2 NPs) to enhance the binding of biomolecules [16]. CeO_2 NPs exhibit unique properties, including high thermal stability, substantial oxygen storage capacity, and biocompatibility [17,18]. The oxidation potential and electronegative oxygen atoms in ceria facilitate interactions

with biomolecules such as proteins and nucleic acids. These properties render ceria suitable for applications as an antibacterial agent, catalyst, therapeutic, medicinal, and biosensor material [19].

Methods for synthesizing CeO_2 NPs include hydrothermal [20], sol-gel [21], and coprecipitation techniques [22]. To control the size of nanoscale cerium oxide particles and prevent agglomeration, a particle size regulation technique is essential. Typically, the use of templates like polyvinyl-pyrrolidone [23] and poly(ethylene glycol) (PEG) polymers assists in synthesizing nanoparticles [24]. These polymers act as surfactants, reducing particle aggregation during deposition, thus allowing for the creation of smaller, more uniform particles [24]. However, despite their effectiveness, incorporating such polymers can have negative environmental impacts [25]. In addition, a diverse variety of organic solvents, including methanol, acetone, ether, benzene, toluene, esters, halogenated, and nitrated hydrocarbons, are widely employed in chemical synthesis. These solvents exhibit high volatility, toxicity, and danger, raising significant concerns for both human health and the environment [26]. The synthesis of NPs *via* environmentally friendly methods enhances the advancement of green electrochemical sensing platforms. This involves the use of non-hazardous solvents and reagents for green synthesis, as well as the production of NPs from waste resources.

Green synthesis is a sustainable method for producing materials that utilize environmentally friendly processes and generates non-toxic by-products. This method often involves biological sources like microorganisms and plants. Studies have shown that green synthesis of nanoceria can be achieved using plant extracts that act as both stabilizing and capping agents [27]. Some examples of such plants include *Aloe barbadensis Mill* [28], Abelmoschus esculentus [29], lemongrass leaves [30], cassava tuber [31], banana peel [32] and even fungi like *Humicola sp.* [33]. The compounds responsible for facilitating this synthesis are typically primary or secondary metabolites found in these biological materials. Orange peels are rich in secondary metabolites, including alkaloids, flavonoids, saponins, tannins, phenols, terpenoids, and steroids, which can inhibit nanoparticle agglomeration [34]. Furthermore, orange peels contain soluble sugars, insoluble polysaccharides, and polyphenols that function as reducing agents, while carboxylic groups, amino acids, and citric acid act as stabilizing agents [35,36]. These components make orange peel extract an effective stabilizer in the CeO_2 NPs synthesis process.

Herein, we report on the electrochemical immunosensor to detect porcine gelatine utilizing green synthesized CeO_2 NPs with orange peel extract as stabilizer.

Experimental

Materials

The materials used for this study included distilled water, *Siamese* orange peel, cerium nitrate hexahydrate [$Ce(NO_3)_3{\times}6H_2O$; Merck, France], ethanol 99.8 % (Merck, France), ammonia (Sigma-Aldrich, Germany), phosphate buffer saline (PBS; pH 7.4; VWR, USA), rabbit anti-porcine gelatine, skin (Polyclonal; Serum; Sigma-Aldrich, Germany), bovine serum albumin (BSA; Sigma-Aldrich, Germany), porcine gelatine (Sigma-Aldrich, Germany), potassium chloride (KCl, Merck, Germany), potassium ferricyanide (III) ($K_3[Fe(CN)_6]$ Sigma-Aldrich, Germany), and SPCE DS 150 (DropSense, Spain) with carbon as working and counter, and silver wire as pseudo-reference electrode.

Instruments

The equipment used in this research included laboratory glassware (Pyrex, Indonesia), a thermometer (GEA, Indonesia), a magnetic stirrer (JOANLAB, China), a hot plate (JOANLAB, China), a centrifuge (Beckman Model TJ-6 Centrifuge, USA), FTIR (Thermo Scientific Type Nicolet iS5, USA),

XRD (Bruker D8 Advance LINXEYE XE-T, Germany), TEM (Hitachi H9500, Japan), PSA (Beckman Coulter LS 13 320, USA), and a potentiostat (Zimmer & Peacock, UK).

Preparation of Siamese orange peel extract

The extraction of *Siamese* orange peel was performed based on a previously reported method [34], with slight modifications. In brief, 100 g of clean orange peel was cut into small pieces and dried in an oven at 60 °C for 24 hours. The dried peel was then soaked in 40 mL of ethanol for 30 minutes and subsequently filtered to obtain the extract. The schematic representation of this extraction process is shown in Figure 1.

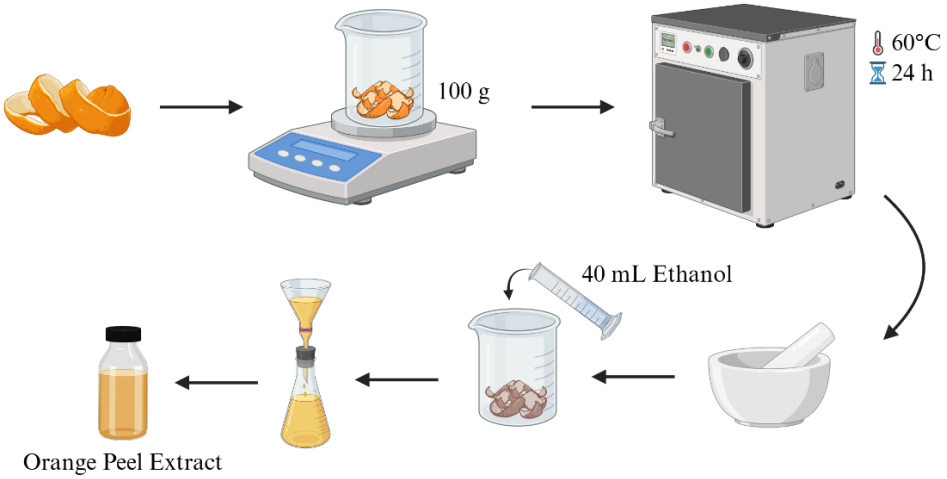

Figure 1. *Schematic of preparation of Siamese orange peel extract*

Synthesis of CeO_2 nanoparticles

Cerium nitrate (1.0605 g) is dissolved in 5 mL of distilled water. Then, 1.5 mL of orange peel extract is added. The solution is stirred for 90 min at 80 °C. Subsequently, 1 M ammonia is added dropwise, and the mixture is stirred for an additional hour. The solution is then centrifuged for 10 min at 10,000 rpm. The resulting precipitate is washed three times with distilled water and ethanol, and then centrifuged under the same conditions. The precipitate is then dried in an oven at 60 °C for 24 hours, followed by calcination at 800 °C for 2 hours. The synthesis of CeO_2 NPs without orange peel follows the same method, except that no orange peel extract is added during the synthesis process.

Characterization of CeO_2 nanoparticles

The synthesized CeO_2 NPs are characterized using transmission electron microscopy (TEM), Fourier transform infrared spectroscopy (FTIR), X-ray diffraction (XRD), particle size analysis (PSA), and electrochemical methods to assess their physicochemical properties.

Drop-casting on screen-printed carbon electrodes

Bare SPCE was modified by drop-casting 10 µL of 100 ppm CeO_2 nanoparticle suspension (equivalent to 1 µg of CeO_2) onto the working area (12.57 mm^2; theoretical loading of CeO_2 per electrode area is 7.96 µg cm^{-2}), followed by drying at room temperature. Then, 10 µL of antibody is added and left to incubate for 30 minutes, followed by rinsing with phosphate buffer saline (PBS) and drying at room temperature. Subsequently, the electrode is incubated with 1 % bovine serum albumin (BSA) for 15 minutes, rinsed with PBS, and dried at room temperature. For sample measurement, the electrode is incubated again with 10 µL of porcine gelatine solution at a specific concentration for 30 minutes. The fabrication steps of the electrochemical immunosensor electrode are illustrated in Figure 2.

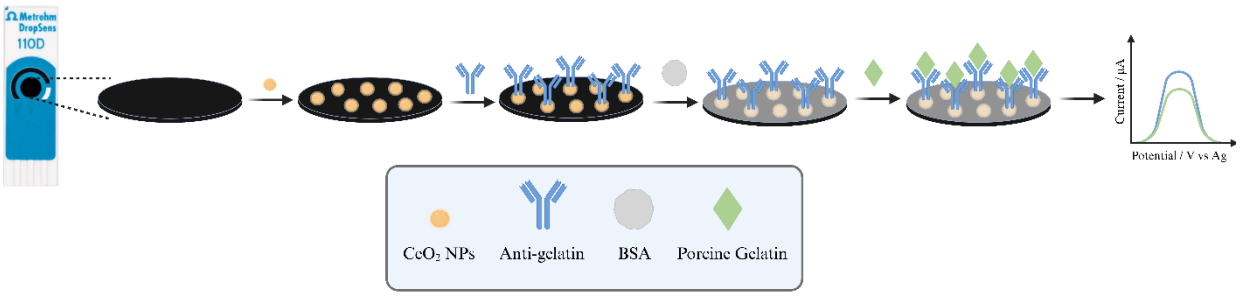

Figure 2. *Schematic of electrochemical immunosensor electrode fabrication*

Electrochemical measurements

The immunosensor is characterized electrochemically using differential pulse voltammetry (DPV) to obtain current values over a potential range of -0.3 to +0.5 V at a scan rate of 8 mV s^{-1}. The step potential (E_{step}) was set at 4 mV with a pulse amplitude (E_{pulse}) of 0.025 V and a pulse time (t_{pulse}) of 0.05 s. All potentials in DPV measurements are reported relative to the $[Fe(CN)_6]^{3-}/[Fe(CN)_6]^{4-}$ redox couple, which also served as an internal reference under measurement conditions using a pseudo-reference Ag electrode printed on the SPCE.

Results and discussion

The synthesized CeO_2 NPs are obtained as a solid with a yellowish-white color. In this synthesis process, the extract of *Siamese* orange peel acts as a stabilizing agent for cerium ions due to the abundance of OH groups from glucose present in the extract. These OH groups can donate electrons, allowing interaction with Ce^{3+} ions in the $Ce(NO_3)_3$ solution. This interaction forms a complex between Ce^{3+} ions and OH groups, resulting in more stable coordination bonds, thus reducing the likelihood of oxidation or precipitation of the ions [31,32,37].

Heating during the synthesis process aims to decompose nitrates from the solution into nitrogen oxide gas and oxygen gas [31]. To control particle size during the core growth process, ammonia needs to be added gradually and consistently. The addition of ammonia creates a basic environment in the solution, allowing Ce(III) to oxidize to Ce(IV) and form $Ce(OH)_4$ precipitate. The final stage of this synthesis process involves drying to remove water and calcination at high temperatures to enhance crystallinity, yielding nanoparticles with high activity by converting $Ce(OH)_4$ into crystalline CeO_2 nanoparticles.

X-ray diffraction (XRD) characterization was performed to determine the crystal characteristics of the synthesized CeO_2 NPs using Cu Kα (λ = 0.154 nm) at 2θ angles ranging from 20 to 80°. The XRD diffractogram is shown in Figure 3(a), and peaks can be observed at 2θ values of 28.4, 32.9, 47.3, 56.2, 58.9, 69.3 and 76.6°, indicating a face-cantered cubic structure, consistent with the reference JCPDS 34-0394. Each peak corresponds to crystal orientation on the planes (111), (200), (220), (311), (222), (400), (331) and (420). These results confirm that the crystals produced through the green synthesis process are CeO_2 crystals, consistent with the reference, with a crystallinity of 77.31 %.

Figure 3(b) shows the FTIR measurement results of CeO_2 NPs synthesized without (green) and with orange peel extract (blue). Both spectra exhibit a peak around 530 cm^{-1} representing Ce-O and O-Ce-O bonds of CeO_2. For CeO_2 NPs using the green synthesis method, new peaks appear at wavelengths of 852 and 1059 cm^{-1}. These peaks likely represent C-O-C stretching from ring vibrations of the orange peel extract used due to its polyphenol content [36].

Particle size analysis (PSA) was conducted to ascertain the particle size of the synthesized CeO_2 dispersion (Table S1, Supplementary material). CeO_2 NPs from green synthesis using orange peel

exhibit smaller sizes compared to synthesis without peel addition. From these results, it can be concluded that orange peel extract influences the agglomeration process of CeO_2 NPs.

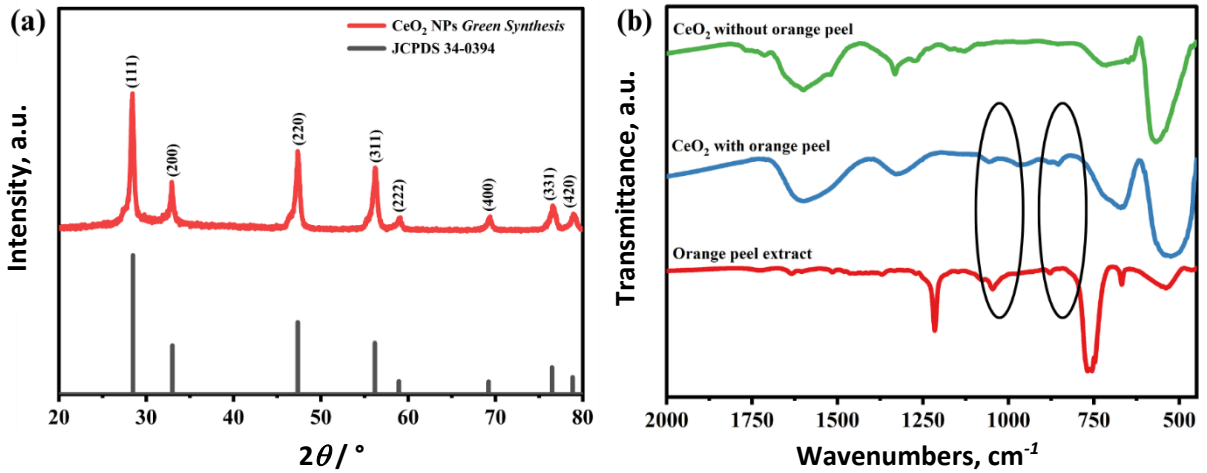

Figure 3. *(a) XRD pattern comparison of CeO_2 NPs and reference. (b) FTIR spectra of CeO_2 NPs without orange peel (green), green synthesis with orange peel (blue), and orange peel extract (red)*

The particle size of CeO_2 NPs was further characterized using TEM. CeO_2 NPs synthesized by the green synthesis method exhibited the characteristic cubic morphology of CeO_2, as shown in Figure 4(a). The actual particle size of the CeO_2 NPs, which is small and uniform, can also be observed from the TEM characterization results. In contrast, the TEM results of CeO_2 NPs without orange peel in Figure 4(b) show larger and more irregular particles. It can be concluded that orange peel extract acts as a stabilizing agent that directs the CeO_2 particle size to be more uniform and prevents agglomeration during the nucleation and growth process. Figure 4(c) shows the particle size distribution graph of each particle resulting from green synthesis. The particle size of CeO_2 NPs with orange peel ranges from 4 to 22 nm, with an average size of 12 nm based on 100 observed particles.

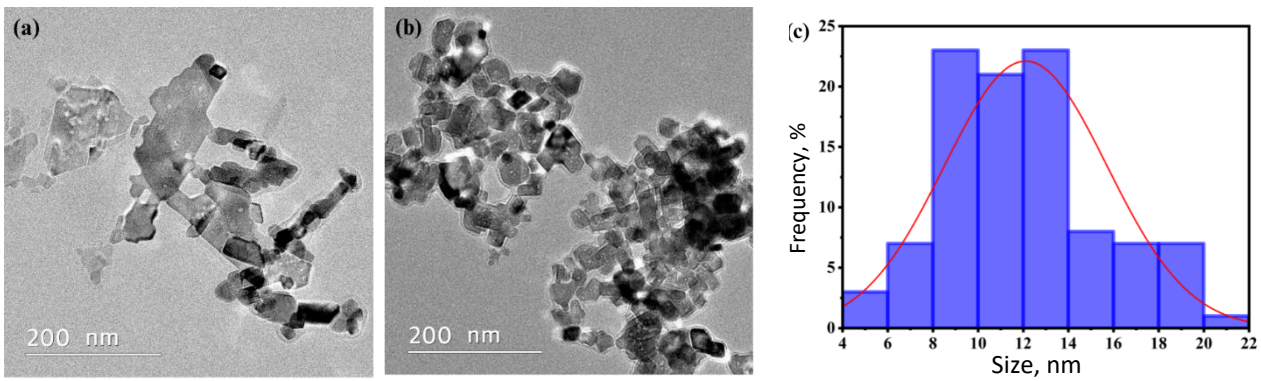

Figure 4. *TEM results of CeO_2 NPs (a) without orange peel and (b) with orange peel. (c) Particle size distribution of CeO_2 NPs with orange peel*

The characterization results using PSA and TEM showed different particle sizes because TEM characterizes CeO_2 NPs in solid form, while PSA characterizes CeO_2 NPs dispersed in a solution. Samples in dispersed form have the potential to agglomerate, which may result in different size measurements [31]. Both characterizations are needed to confirm the size of the CeO_2 NPs formed with and without a dispersing medium to understand the characteristics of the produced nanoparticles.

The synthesized CeO_2 NPs were used to modify SPCE using the drop-cast method for the detection of porcine gelatine. The modified SPCE was immobilized with anti-porcine gelatine and porcine gelatine. Each stage of electrode modification and biomolecule immobilization, including the drop-

cast of CeO_2 NPs, immobilization of anti-porcine gelatine, blocking with bovine serum albumin (BSA) and interaction with porcine gelatine, was characterized using DPV, based on the redox response of the $[Fe(CN)_6]^{3-}/[Fe(CN)_6]^{4-}$, which is sensitive to changes in surface properties, particularly those that affect electron transfer kinetics. DPV characterization showed a decrease in peak current due to the hindered electron transfer on the electrode surface caused by the immobilization of large biomolecules, indicating that the immobilization step was successful (Figure 5). CeO_2 NPs have been reported to bind with antibodies without the addition of other agents, allowing more antibodies to bind to the electrode [15]. These nanoparticles are particularly suitable for immobilization of biorecognition elements due to their favourable surface chemistry, which enables covalent bonding through amine groups and residual cysteine present in biomolecules, such as anti-porcine gelatine [38]. In addition to their ability to form covalent bonds, CeO_2 NPs exhibit a high isoelectric point (approximately 9.2), resulting in a positively charged surface under physiological pH conditions. This characteristic promotes strong electrostatic interactions with negatively charged biomacromolecules, such as antibodies, which typically possess lower isoelectric points [39,40]. Furthermore, CeO_2 NPs possess abundant crystal defects, redox-active Ce^{3+}/Ce^{4+} states, and a high oxygen storage capacity, all of which contribute to enhanced surface reactivity and coordination ability, making them an excellent platform for stable and efficient biomolecule immobilization [41]. Subsequently, the anti-porcine gelatine attached to the electrode can bind to the target gelatine in a lock-and-key manner. The interactions involved are non-covalent bonds such as hydrogen bonds, electrostatic interactions, and van der Waals bonds that occur specifically between proteins and their ligands [2].

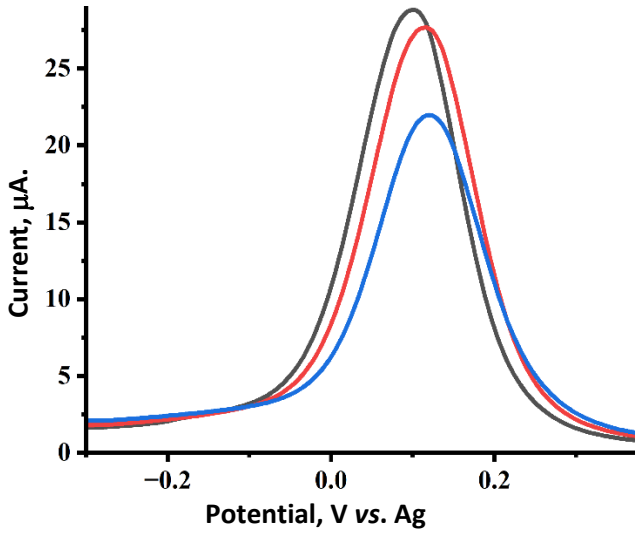

Figure 5. *DPV characterization results of SPCE bare (black), SPCE/CeO_2/AntiG (red), SPCE/CeO_2/AntiG/Gelatine (blue) in 0.1 M KCl containing 0.01 M $K_3[Fe(CN)_6]$ solution within the potential range of -0.3 to +0.5 V with E_{step} = 4 mV; E_{pulse} = 25 mV; t_{pulse} = 0.05 s; scan rate: 8 mV s^{-1}. The porcine gelatine-was 10 ppm*

Before immobilization with porcine gelatine, the electrode was incubated with 1 % BSA to cover the unmodified active sites of the electrode, thereby reducing interference in the measurement results. Figure 5 shows a decrease in current when 10 ppm porcine gelatine is added, as porcine gelatine is a large, non-electroactive biomolecule that hinders electron transfer processes on the electrode surface.

Table 1 shows a greater decrease in current response (Δi / %) for gelatine for SPCE modified with CeO_2 NPs synthesized *via* green synthesis with orange peel extract. The change in Δi refers to the decrease in current when the target analyte is introduced, compared to the baseline current (blank).

This value is obtained by subtracting the current measured in the presence of the target from the blank current, then dividing the result by the blank current, and finally multiplying by 100 to express it as a percentage. This indicates that the use of orange peel can enhance the performance of the electrochemical biosensor for detecting porcine gelatine. The corresponding DPV voltammograms are provided in the supplementary material (Figure S1).

Table 1. *Comparison of Δi in CeO_2 NPs synthesized with and without orange peel*

Synthesis results	Description	Current, μA	Δ*i* / %
Without orange peel	blank	23.21	4.98
	target	22.05	
With orange peel	blank	23.84	15.37
	target	20.17	

Next, the concentration of CeO_2 NPs immobilized on the electrode surface was optimized. The related DPV voltammograms for different concentrations are provided in Figure S2. Table 2 shows that the concentration of CeO_2 NPs with the highest Δ*i* is 100 ppm. Δ*i* reflects the amount of target proportional to its concentration. It can be observed that without the addition of CeO_2 NPs (0 ppm), there is no decrease in current from the sample. This demonstrates that the proposed electrochemical immunosensor cannot detect gelatine without the assistance of CeO_2 NPs binding the antibody bioreceptor to the electrode surface. This Δ*i* is then used to assess the response change across various target concentrations (Figure 6a), resulting in the calibration curve for gelatine target depicted in Figure 6b. The linearity achieved is represented by the regression equation $y = 1.3568x +$ + 2.1408 with $R^2 = 0.9912$. The LOD obtained in this measurement is 3.53 ppm.

Table 2. *Comparison of Δi at different concentrations of CeO_2 NPs*

Concentration, ppm	Description	Current, μA	Δ*i* / %
0	blank	21.42	-
	target	23.98	
100	blank	23.56	16.66
	target	19.63	
300	blank	22.79	12.58
	target	19.92	

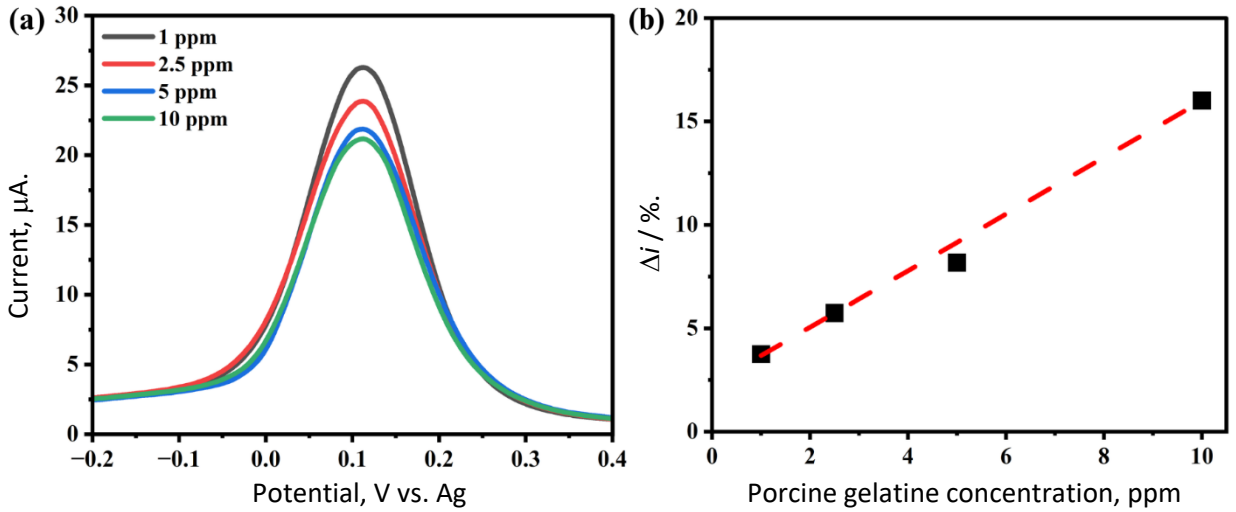

Figure 6. *(a) DPV voltammograms of porcine gelatine concentrations (1, 2.5, 5 and 10 ppm) in 0.1 M KCl containing 0.01 M $K_3[Fe(CN)_6]$ solution within the potential range of -0.3 to +0.5 V with E_{step} = 4 mV; E_{pulse} = 25 mV; t_{pulse} = 0.05 s; scan rate: 8 mV s^{-1}. (b) Calibration curve of the electrochemical immunosensor for detecting porcine gelatine*

Selectivity was assessed by comparing the immunosensor's response to commercial bovine gelatine under the same conditions. The comparison of DPV voltammograms between commercial bovine gelatine and porcine gelatine is shown in Figure 7. Table S2 shows that the Δ*i* of commercial porcine gelatine samples is higher compared to commercial bovine gelatine, with a selectivity for porcine gelatine of 67.48 %. These results demonstrate that the modified electrode can specifically detect commercial porcine gelatine, as evidenced by the markedly higher signal resulting from the selective binding of anti-porcine gelatine antibodies. The present findings could serve as a preliminary step in verifying the halal status of a food product.

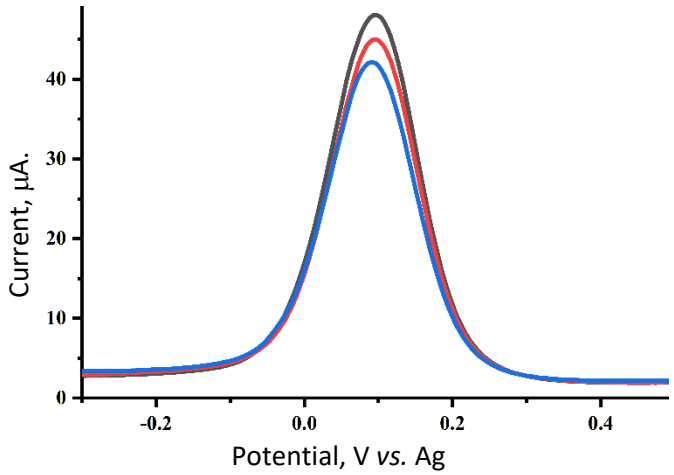

Figure 7. *DPV characterization results of SPCE/CeO_2/AntiG/blank (black), SPCE/CeO_2/AntiG/bovinegelatine (red), SPCE/Ceria/AntiG/porcinegelatine (blue) in 0.1 M KCl containing 0.01 M $K_3[Fe(CN)_6]$ solution within the potential range of -0.3 to +0.5 V with* E_{step} *= 4 mV;* E_{pulse} *= 25 mV;* t_{pulse} *= 0.05 s; scan rate: 8 mV* s^{-1}

Conclusions

This study successfully demonstrates the green synthesis of CeO_2 NPs using Siamese orange peel extract, producing nanoparticles with a cubic morphology, an average particle size of 12 nm, and a crystallinity of 77.31 %. The use of orange peel extract as a stabilizing agent effectively prevented nanoparticle agglomeration, resulting in uniform and well-dispersed CeO_2 NPs suitable for electrochemical applications. The synthesized CeO_2 NPs were utilized to modify SPCE, enhancing the immobilization of bioreceptors for the electrochemical immunosensor detection of porcine gelatine. The developed sensor exhibited a limit of detection of 3.53 ppm with a selectivity of 67.48 % for porcine gelatine, demonstrating its potential for accurate food authentication. These findings highlight the effectiveness of green-synthesized CeO_2 NPs in improving biosensor performance while promoting environmentally friendly material synthesis, contributing to the advancement of sustainable and sensitive electrochemical sensing platforms for food safety monitoring.

Supplementary material: *Additional data are available electronically on article page of the journal's website: https://pub.iapchem.org/ojs/index.php/JESE/article/view/2698, or from the corresponding author upon request.*

Acknowledgements*: Authors would like to thank the Ministry of Education, Culture, Research, and Technology (Kemendikbudristek) for organizing PKM 2024 and supporting the research. Authors also thank Universitas Padjadjaran for providing the opportunity and research funding, which enabled the development of research that can be used for educational and research activities. Authors acknowledge E-Layanan Sains, BRIN, for the support of laboratory instrument facilities.*

References

[1] M. Momtaz, S. Y. Bubli, M. S. Khan, Mechanisms and Health Aspects of Food Adulteration: A Coprehensive Review, *Foods* **12** (2023) 199. https://doi.org/10.3390/foods12010199

[2] J.A. Rather, N. Akhter, Q. S. Ashraf, S. A. Mir, H. A. Makroo, D. Majid, F. J. Barba, A. M. Khaneghah, B. N. Dar, A comprehensive review on gelatin: Understanding impact of the sources, extraction methods, and modifications on potential packaging applications, *Food Packaging and Shelf Life* **34** (2022) 100945. https://doi.org/10.1016/j.fpsl.2022.100945

[3] N. García, M. Hernández, M. Gutierrez-Boada, A. Valero, A. Navarro, M. Muñoz-Chimeno, A. Fernández-Manzano, F.M. Escobar, I. Martínez, C. Bárcena, S. González, A. Avellón, J.M. Eiros, G. Fongaro, L. Domínguez, J. Goyache, D. Rodríguez-Lázaro, Occurrence of Hepatitis E Virus in Pigs and Pork Cuts and Organs at the Time of Slaughter, Spain, 2017, *Frontiers in Microbiology* **10** (2020) 2990. https://doi.org/10.3389/fmicb.2019.02990

[4] E. Bilska-Zając, M. Różycki, E. Antolak, A. Bełcik, K. Grądziel-Krukowska, J. Karamon, J. Sroka, J. Zdybel, T. Cencek, Occurrence of *Trichinella* spp. in rats on pig farms, *Annals of Agricultural and Environmental Medicine* **25** (2018) 698-700. https://doi.org/10.26444/aaem/99555

[5] X. Zhu, S. Gu, D. Guo, X. Huang, N. Chen, B. Niu, X. Deng, Determination of porcine derived components in gelatin and gelatin-containing foods by high performance liquid chromatography-tandem mass spectrometry, *Food Hydrocolloids* **134** (2023) 107978. https://doi.org/10.1016/j.foodhyd.2022.107978

[6] N. Salamah, Y. Erwanto, S. Martono, A. Rohman, The Employment of Real-Time Polymerase Chain Reaction Using Species-Specific Primer Targeting on D-Loop Mitochondria for Identification of Porcine Gelatin in Soft Candy, *Indonesian Journal of Chemistry* **21** (2021) 852-859. https://doi.org/10.22146/ijc.60413

[7] S. M. K. Uddin, M. A. M. Hossain, Z. Z. Chowdhury, M. R. Bin Johan, Short targeting multiplex PCR assay to detect and discriminate beef, buffalo, chicken, duck, goat, sheep and pork DNA in food products, *Food Additives & Contaminants A* **38** (2021) 1273-1288. https://doi.org/10.1080/19440049.2021.1925748

[8] H. M. Hassan, U. D. Souka, S. M. Hassan, Differentiation and quantification of bovine and pork gelatin using UPLC-QTOF and ATR-FTIR spectroscopy: Addressing challenges in mixed gelatin analysis and detection, *Food Chemistry* **464** (2025) 141883. https://doi.org/10.1016/j.foodchem.2024.141883

[9] Q. Zia, M. Alawami, N. F. K. Mokhtar, R. M. H. R. Nhari, I. Hanish, Current analytical methods for porcine identification in meat and meat products, *Food Chemistry* **324** (2020) 126664. https://doi.org/10.1016/j.foodchem.2020.126664

[10] J. Du, M. Gan, Z. Xie, C. Zhou, M. Li, M. Wang, H. Dai, Z. Huang, L. Chen, Y. Zhao, L. Niu, S. Zhang, Z. Guo, J. Wang, X. Li, L. Shen, L. Zhu, Current progress on meat food authenticity detection methods, *Food Control* **152** (2023) 109842. https://doi.org/10.1016/j.foodcont.2023.109842

[11] J. Kim, M. Park, Recent Progress in Electrochemical Immunosensors, *Biosensors* **11** (2021) 360. https://doi.org/10.3390/bios11100360

[12] F. Bettazzi, G. Marrazza, M. Minunni, I. Palchetti, S. Scarano, Biosensors and Related Bioanalytical Tools, *Comprehensive Analytical Chemistry* **77** (2017) 1-33. https://doi.org/10.1016/bs.coac.2017.05.003

[13] L. Meng, S. Chirtes, X. Liu, M. Eriksson, W. C. Mak, A green route for lignin-derived graphene electrodes: A disposable platform for electrochemical biosensors, *Biosensors and Bioelectronics* **218** (2022) 114742. https://doi.org/10.1016/J.BIOS.2022.114742

[14] G. Paimard, E. Ghasali, M. Baeza, Screen-Printed Electrodes: Fabrication, Modification, and Biosensing Applications, *Chemosensors* **11** (2023) 113. https://doi.org/10.3390/chemosensors11020113
[15] Y. W. Hartati, D. R. Komala, D. Hendrati, S. Gaffar, A. Hardianto, Y. Sofiatin, H. H. Bahti, An aptasensor using ceria electrodeposited-screen-printed carbon electrode for detection of epithelial sodium channel protein as a hypertension biomarker, *Royal Society Open Science* **8** (2021) 202040. https://doi.org/10.1098/rsos.202040
[16] R. Chetty, M. Singh, In-vitro interaction of cerium oxide nanoparticles with hemoglobin, insulin, and dsDNA at 310.15 K: Physicochemical, spectroscopic and in-silico study, *International Journal of Biological Macromolecules* **156** (2020) 1022-1044. https://doi.org/10.1016/j.ijbiomac.2020.03.067
[17] Z. Chen, Y. Xie, K. Li, L. Huang, X. Zheng, Synthesis of carbon coated-ceria with improved cytocompatibility, *Ceramics International* **45** (2019) 19981-19990. https://doi.org/10.1016/j.ceramint.2019.06.256
[18] W. X. Tang, P. X. Gao, Nanostructured cerium oxide: Preparation, characterization, and application in energy and environmental catalysis, *MRS Communications* **6** (2016) 311-329. https://doi.org/10.1557/mrc.2016.52
[19] S. N. Zakiyyah, D. R. Eddy, M. L. Firdaus, T. Subroto, Y. W. Hartati, Screen-printed carbon electrode/natural silica-ceria nanocomposite for electrochemical aptasensor application, *Journal of Electrochemical Science and Engineering* **12** (2022) 1225-1242. https://doi.org/10.5599/jese.1455
[20] C. Maria Magdalane, K. Kaviyarasu, B. Siddhardha, G. Ramalingam, Synthesis and characterization of CeO_2 nanoparticles by hydrothermal method, *Materials Today: Proceedings* **36** (2021) 130-132. https://doi.org/10.1016/j.matpr.2020.02.283
[21] L. D. Sonawane, A. S. Mandawade, L. N. Bhoye, H. I. Ahemad, S. S. Tayade, Y. B. Aher, A. B. Gite, L. K. Nikam, S. D. Shinde, G. H. Jain, G. E. Patil, M. S. Shinde, Sol-gel and hydrothermal synthesis of CeO_2 NPs: Their physiochemical properties and applications for gas sensor with photocatalytic activities, *Inorganic Chemistry Communications* **164** (2024) 112313. https://doi.org/10.1016/j.inoche.2024.112313
[22] M. Farahmandjou, M. Farahmandjou, M. Zarinkamar, T. P. Firoozabadi, Synthesis of Cerium Oxide (CeO_2) nanoparticles using simple CO-precipitation method, *Revista Mexicana de Física* **62** (2016) 496-499. https://www.scielo.org.mx/scielo.php?script=sci_arttext&pid=S0035-001X2016000500496
[23] A. A. Baqer, K. A. Matori, N. M. Al-Hada, A. H. Shaari, E. Saion, J. L. Y. Chyi, Effect of polyvinylpyrrolidone on cerium oxide nanoparticle characteristics prepared by a facile heat treatment technique, *Results in Physics* **7** (2017) 611-619. https://doi.org/10.1016/j.rinp.2017.01.020
[24] Y. Rehman, H. Qutaish, J. H. Kim, X. F. Huang, K. Konstantinov, Nanoarchitectonics of (110) directed polyethylene glycol stabilized cerium nanoparticles for UV filtering applications, *Journal of Mateials Science* **57** (2022) 12848-12864. https://doi.org/10.1007/s10853-022-07437-9
[25] Y. S. Ridwan, Y. W. Hartati, M. Sriariyanun, A. A. Septevani, Progressions in Modified Graphite Electrodes with Green Nanostructured Materials for Low Cost and Sustainable Electrochemical Detection of Environmental Contaminants, *Applied Science and Engineering Progress* **18** (2025) 7630. https://doi.org/10.14416/j.asep.2024.10.006
[26] P. K. Kalambate, Z. Rao, Dhanjai, J. Wu, Y. Shen, R. Boddula, Y. Huang, Electrochemical (bio) sensors go green, *Biosensors and Bioelectronics* **163** (2020) 112270. https://doi.org/10.1016/j.bios.2020.112270

[27] A. Iqbal, A. S. Ahmed, N. Ahmad, A. Shafi, T. Ahamad, M. Z. Khan, S. Srivastava, Biogenic synthesis of CeO_2 nanoparticles and its potential application as an efficient photocatalyst for the degradation of toxic amido black dye, *Environmental Nanotechnology, Monitoring & Management* **16** (2021) 100505. https://doi.org/10.1016/j.enmm.2021.100505

[28] B. N. Raj, P. N. T. Gowda, O. S. Pooja, S. K. Sukrutha, B. Purushotham, H. P. Nagaswarupa, M. R. Anil Kumar, B. S. Surendra, S. T. R. Shekhar, S. C. Prashantha, Eco-friendly synthesis of CeO_2 NPs using *Aloe barbadensis Mill* extract: Its biological and photocatalytic activities for industrial dye treatment applications, *Journal of Photochemistry and Photobiology* **7** (2021) 100038. https://doi.org/10.1016/j.jpap.2021.100038

[29] H. E. Ahmed, Y. Iqbal, M. H. Aziz, M. Atif, Z. Batool, A. Hanif, N. Yaqub, W. A. Farooq, S. Ahmad, A. Fatehmulla, H. Ahmad, Green Synthesis of CeO_2 Nanoparticles from the *Abelmoschus esculentus* extract: Evaluation of antioxidant, anticancer, antibacterial, and wound-Healing Activities, *Molecules* **26** (2021) 4659. https://doi.org/10.3390/molecules26154659

[30] S. Maensiri, S. Labuayai, P. Laokul, J. Klinkaewnarong, E. Swatsitang, Structure and optical properties of CeO_2 nanoparticles prepared by using lemongrass plant extract solution, *Japanese Journal of Applied Physics* **53** (2014) 06JG14. https://doi.org/10.7567/JJAP.53.06JG14

[31] S. N. Zakiyyah, N. Irkham, Y. Einaga, N. S. Gultom, R. P. Fauzia, G. T. M. Kadja, S. Gaffar, M. Ozsoz, Y. W. Hartati, Green Synthesis of Ceria Nanoparticles from Cassava Tubers for Electrochemical Aptasensor Detection of SARS-CoV-2 on a Screen-Printed Carbon Electrode, *ACS Applied Bio Materials* **7** (2024) 2488-2498. https://doi.org/10.1021/acsabm.4c00088

[32] A. Miri, H. Beiki, A. Najafidoust, M. Khatami, M. Sarani, Cerium oxide nanoparticles: green synthesis using Banana peel, cytotoxic effect, UV protection and their photocatalytic activity, *Bioprocess and Biosystems Engineering* **44** (2021) 1891-1899. https://doi.org/10.1007/s00449-021-02569-9

[33] S. A. Khan, A. Ahmad, Fungus mediated synthesis of biomedically important cerium oxide nanoparticles, *Materials Research Bulletin* **48** (2013) 4134-4138. https://doi.org/10.1016/j.materresbull.2013.06.038

[34] M. S. Irshad, M. H. Aziz, M. Fatima, S. U. Rehman, M. Idrees, S. Rana, F. Shaheen, A. Ahmed, M. Q. Javed, Q. Huang, Green synthesis, cytotoxicity, antioxidant and photocatalytic activity of CeO_2 nanoparticles mediated via orange peel extract (OPE), *Materials Research Express* **6** (2019) 0950a4. https://doi.org/10.1088/2053-1591/AB3326

[35] M. M. Abomughaid, Bio-Fabrication of Bio-Inspired Silica Nanomaterials from Orange Peels in Combating Oxidative Stress, *Nanomaterials* **12** (2022) 3236. https://doi.org/10.3390/nano12183236

[36] M. Rehan, N.A.M. Abdel-Wahed, A. Farouk, M.M. El-Zawahry, Extraction of Valuable Compounds from Orange Peel Waste for Advanced Functionalization of Cellulosic Surfaces, *ACS Sustainable Chemistry & Engineering* **6** (2018) 5911-5928. https://doi.org/10.1021/acssuschemeng.7b04302

[37] M. Darroudi, M. Hakimi, M. Sarani, R. Kazemi Oskuee, A. Khorsand Zak, L. Gholami, Facile synthesis, characterization, and evaluation of neurotoxicity effect of cerium oxide nanoparticles, *Ceramics International* **6** (2013) 6917-6921. https://doi.org/10.1016/J.CERAMINT.2013.02.026

[38] R. A. C. Amoresi, N. A. V. Roza, T. Mazon, Applying CeO_2 nanorods in flexible electrochemical immunosensor to detect C-reactive protein, *Journal of Electroanalytical Chemistry* **935** (2023) 117353. https://doi.org/10.1016/J.JELECHEM.2023.117353

[39] A. A. Ansari, A. Kaushik, P. R. Solanki, B. D. Malhotra, Nanostructured zinc oxide platform for mycotoxin detection, *Bioelectrochemistry* **77** (2010) 75-81. https://doi.org/10.1016/J.BIOELECHEM.2009.06.014

[40] A. A. Ansari, R. Lv, A. K. Parchur, M. Dhayal, Enhancing biosensor sensitivity with CeO_2 nanocomposites for biomedical and environmental applications, *Chemical Engineering Journal* **512** (2025) 162526. https://doi.org/10.1016/J.CEJ.2025.162526

[41] N. Ahmad, M. Alam, R. Wahab, J. Ahmad, M. Ubaidullah, A. A. Ansari, N. M. Alotaibi, Synthesis of NiO-CeO_2 nanocomposite for electrochemical sensing of perilous 4-nitrophenol, *Journal of Materials Science: Materials in Electronics* **30** (2019) 17643-17653. https://doi.org/10.1007/s10854-019-02113-2